Separation and Purification Technology 194 (2018) 410–415

Contents lists available at ScienceDirect

Separation and Purification Technology

journal homepage: www.elsevier.com/locate/seppur

Short Communication

Adsorption and capacitive regeneration of nitrate using inverted capacitive deionization with surfactant functionalized carbon electrodes

Diego I. Oyarzun[a,1], Ali Hemmatifar[a,1], James W. Palko[a,b], Michael Stadermann[c], Juan G. Santiago[a,*]

[a] Department of Mechanical Engineering, Stanford University, Stanford, CA 94305, USA
[b] Department of Mechanical Engineering, University of California, Merced, CA 95340, USA
[c] Lawrence Livermore National Laboratory, 7000 East Avenue, Livermore, CA 94550, USA

ARTICLE INFO

Keywords:
Nitrate removal
Inverted capacitive deionization
Chemical surface charge
Surfactant treatment

ABSTRACT

Nitrate is a pollutant present in groundwater worldwide. Several techniques are available to remove nitrate from water, but they are difficult to automate in remote settings or require chemicals for treatment for regeneration. Here, we demonstrate the use of two surfactant-treated high surface area porous electrodes for passive adsorption of nitrate followed by electrical regeneration. In order to generate the surface charge driving adsorption, we functionalized the active electrode (cathode) and capacitive counter electrode (anode) with cetrimonium bromide (CTAB) and sodium dodecyl benzene sulphonate (SDBS), respectively. We find voltage applied during regeneration is directly proportional to the subsequent available adsorption capacity at short circuit. In a recent preliminary work, we used a Faradaic counter electrode, and here, we compare both studies in terms of energy-normalized adsorbed salt (*ENAS*)—a measure of energy efficiency—and average salt adsorption rate (*ASAR*). We show that capacitive counter electrode used in this work increases *ENAS* by two orders of magnitude, while maintaining a similar *ASAR*.

1. Introduction

Nitrate (NO_3^-) is a contaminant of growing concern that affects water quality globally. Intensification of agricultural activities has led to a growth in the use of fertilizers, which are increasing nitrate levels in groundwater and disturbing the balance in the nitrogen cycle [1,2]. Nitrate indirectly produces health hazards by reduction to toxic nitrite in the human digestive system. Moreover, infants are susceptible to developing methemoglobinemia when exposed to high levels of nitrate [3–6].

Nitrate contamination in groundwater is often diffusely spread over large areas, making point-of-entry or point-of-use systems the most compatible methods for nitrate treatment [7]. Ion exchange is a popular method of treatment in such settings [8,9]. In this method, resins are functionalized with charged groups weakly bound to relatively low affinity ions (e.g. Cl^-). Upon exposure to a solution with higher affinity ions (e.g. NO_3^-), these exchange with the lower affinity ions and are removed from the solution. For example, resins functionalized with trimethyl quaternary amine groups have been shown to have affinity for nitrate [10,11]. Reverse osmosis systems are also effective for nitrate removal from drinking water [12,13]; however, they suffer from high costs and poor water use efficiency [14]. Biological methods are effectively applied for nitrate removal from waste water but not commonly for drinking water [15,16].

Capacitive deionization (CDI) is another method to remove toxic ions from water [17–19]. CDI typically uses a potential to electrostatically adsorb/discharge ions onto/from high surface area electrodes [20]. The product of CDI is purified water during adsorption and a waste stream with high concentration of contaminants during discharge. CDI cells can be used with ion selective membranes to improve charge efficiency [21–23], or without membranes in flow-between or flow-through electrode configurations [20,24,25]. In “traditional” CDI, ions are adsorbed upon application of an external voltage (around 1 V). However, it is possible to adsorb ions onto the electrodes without external voltage by the action of chemical charges on the electrode surfaces. In this operational mode, application of a potential regenerates the CDI cell (ion expulsion) in a process named inverted CDI (i-CDI) [26–29]. Nitrate removal has been demonstrated using traditional CDI (adsorption of nitrate under an applied voltage) with carbon electrodes alone [30,31] or with ion selective membranes [32–34].

* Corresponding author.
E-mail address: juan.santiago@stanford.edu (J.G. Santiago).
[1] Contributed equally.

https://doi.org/10.1016/j.seppur.2017.11.027
Received 27 June 2017; Received in revised form 28 October 2017; Accepted 11 November 2017
Available online 14 November 2017
1383-5866/ © 2017 Elsevier B.V. All rights reserved.

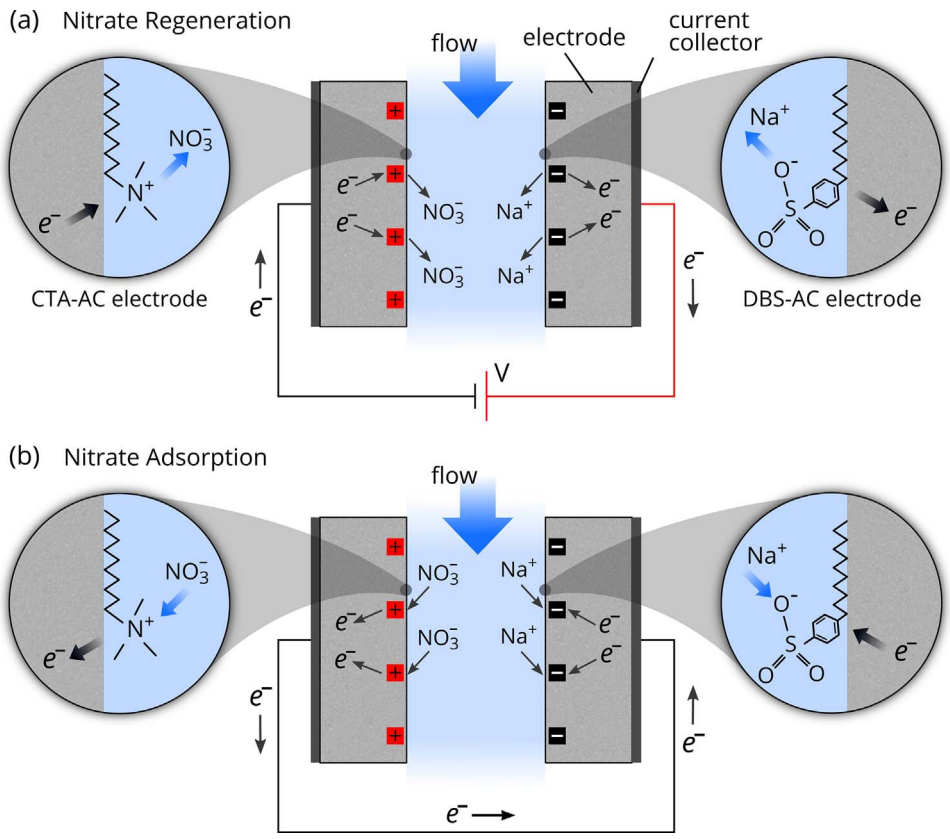

Fig. 1. (a) Schematic of i-CDI cell which features constant voltage regeneration of a passive nitrate adsorber. Negative electrode (CTA-AC) is treated with cetrimonium bromide (CTAB) and positive electrode (DBS-AC) with sodium dodecyl benzene sulphonate (SDBS). The external voltage forces electrons to flow from DBS-AC to CTA-AC, repelling Na^+ and NO_3^- ions from their respective electrodes. Higher voltages enhance the regeneration process and form more positively charged sites on CTA-AC for the subsequent nitrate adsorption step. (b) Schematic of short circuit adsorption process. Na^+ and NO_3^- ions are adsorbed, forcing migration of electrons from CTA-AC to DBS-AC.

In a previous work [35], we took advantage of well-established nitrate affinity of trimethyl quaternary amines for nitrate sequestration [10,11]. To this end, we fabricated a cell with activated carbon (AC) electrodes functionalized with cetrimonium bromide (CTAB) cationic surfactant. The cell consisted of 3.5 cm diameter 300 μm thick CTAB-treated carbon electrode and a second, Faradaic electrode comprised of a single 50 μm thick titanium sheet. A solution of 200 ppm $NaNO_3$ at 0.43 ml min^{-1} flowrate was fed to the cell. We showed that surface charge generated by CTAB leads to nitrate adsorption in the active electrode without applied potential (~80 mg $NaNO_3$ per g of activated carbon). We then regenerated the adsorbed ions by application of 3 V potential to the functionalized electrode. Unlike the current i-CDI cell, the circuit associated with regeneration of the active electrode of that preliminary cell was completed via Faradaic reactions on the titanium electrode.

Fig. 1 shows our current cell which uses two (capacitive) porous electrodes. Relative to our previous work, we replaced the inert titanium electrode with a surfactant-functionalized capacitive counter electrode. Similar to our previous work, we functionalized the active/adsorbing electrode using CTAB. CTAB imparts a positively charged surface for adsorption of nitrate [36]. We functionalized the capacitive counter electrode (also activated carbon) with a sodium dodecyl benzene sulphonate (SDBS) anionic surfactant. The latter treatment creates a negative surface charge to passively adsorb cations at short circuit (Fig. 1b). Throughout this paper, we refer to these active and counter activated carbon (AC) porous electrodes as CTA-AC and DBS-AC, respectively. During adsorption, NO_3^- and counter ions (Na^+ ions here) are adsorbed to their respective electrodes, while electrons migrate from CTA-AC to DBS-AC. As in i-CDI, we remove the adsorbed ions by application of an external voltage to the electrodes (Fig. 1a). The resulting electric field drives electrons from DBS-AC to CTA-AC, repelling Na^+ and NO_3^- ions. We here demonstrate successful nitrate removal (up to more than 10 mg sodium nitrate per g of both electrodes) with our i-CDI system. Relative to our preliminary work [35], this work shows we can replace the Faradaic titanium counter electrode with an SDBS-treated capacitive counter electrode to create a complete i-CDI cell. As we shall see, the current design increases the energy efficiency of nitrate removal (measure by energy-normalized adsorbed salt (*ENAS*) metric) by 1 to 2 orders of magnitude for a similar average salt adsorption rate (*ASAR*).

2. Materials and methods

2.1. Surfactant treatment of electrode material and capacitive counter electrode

Commercially available activated carbon electrodes (Material Methods LLC., PACMM™ 203, Irvine, CA) were used as the active porous carbon electrode and capacitive counter electrode. We functionalized the active electrode (cathode) with trimethyl quaternary amine moieties by adsorption of CTAB surfactant. To this end, we soaked 0.15 g of pristine activated carbon electrode in 500 mL aqueous solution of 10 mM CTAB and 10 mM NaCl overnight and then rinsed thoroughly with deionized (DI) water and dried. We performed a similar functionalization on the capacitive counter electrode with SDBS surfactant. We soaked 0.15 g of pristine activated carbon electrode in 500 mL aqueous solution of 10 mM SBDS and 10 mM NaCl overnight, rinsed with DI water, and dried. We refer to active and counter porous electrodes as CTA-AC and DBS-AC, respectively.

We measured electrical resistance of the electrodes with four-point probe method (Keithley 2400, Cleveland, OH). Upon surface treatment, resistance of uncompressed CTA-AC and DBS-AC electrodes increased respectively about 70% and 20% (from 7.4 Ω cm for untreated carbon to values of 12.5 and to 8.9 Ω cm, respectively). We also experimentally investigated the nitrate affinity of CTAB-treated activated carbon in presence of chloride anions, and describe this in more detail in Section S-1 of the SI.

2.2. Experimental setup

The general experimental setup is described in detail by Palko et al. [35] and the specific implementation in this work is summarized here. It consisted of a radial inflow geometry desalination cell [37], a reservoir with 200 ppm (~2.35 mM) sodium nitrate ($NaNO_3$) solution, a sourcemeter (Keithley 2400, Cleveland, OH), a peristaltic pump (Ismatec IPC-4, Wertheim, Germany), and a flow-through conductivity meter (eDAQ, Denistone East, Australia). The cell consisted of a pair of ~300 μm thick electrodes (one CTA-AC and one DBS-AC) stacked between two 50 μm thick titanium sheet current collectors. A 300 μm thick woven plastic mesh (McMaster-Carr, Los Angeles, CA) was used as spacer between the electrodes. The electrodes had 3.5 cm outer diameter with 0.3 g total dry mass. We used 0.45 mL min^{-1} flow rate and measured effluent conductivity with the conductivity meter. Upon surfactant treatment, we used our desalination cell with CTA-AC and DBS-AC electrodes for cyclic nitrate removal. To explore the relationship between applied potential and regeneration capacity of nitrate, we operated the cell at constant voltage (rather than constant current) operation and with pure sodium nitrate solution. Hence, we applied 0 V for adsorption (short circuit adsorption) and 0.2–1.4 V (with 0.2 V increments) for the regeneration step. Duration of adsorption and regeneration steps was 2 h each.

3. Results and discussion

3.1. Adsorption and electrical regeneration of functionalized activated carbon

Fig. 2 shows measured effluent concentration of $NaNO_3$ and external current for selected cycles with short circuit (at 0 V) adsorption and 0.2, 0.4, 0.6, 0.8, 1, and 1.2 V regeneration steps. Inflow stream was 200 ppm $NaNO_3$ solution at 0.45 mL min^{-1} flow rate. The effluent concentration and electric current for cycles with increasing and decreasing order of regeneration voltages show very similar behavior (see Fig. 2). Upon application of voltage to the cell (negative voltage to CTA-AC and positive voltage to DBS-AC), the surfactant-bound Na^+ and NO_3^- ions are repelled from their respective electrodes. High effluent concentration in regeneration is indicative of this repulsion. Results show an apparent increase in concentration baseline for voltages higher than ~1 V. We attribute this shift mainly to effluent pH fluctuations due to Faradaic reactions [38]. Subsequent to the regeneration, upon short circuit in the adsorption step, electrons in CTA-AC electrode (active electrode) discharge into DBS-AC electrode and the electric current is reversed. Migration of electrons from CTA-AC to DBS-AC is balanced with adsorption of NO_3^- and Na^+ ions from flow stream into CTA-AC and DBS-AC, respectively. These fluxes lower the measured effluent concentration during the adsorption step. Note that in contrast to our preliminary work, [35] the regeneration step here is primarily capacitive (and not Faradaic) at voltages lower than about 1 V. This improves overall energy efficiency for nitrate removal (see Section 3.2), as Faradaic reactions here are insignificant compared to the previous use of a 3 V regeneration with a titanium Faradaic counter electrode (see [35] for more details).

3.2. Treatment of counter electrode is crucial for nitrate regeneration

We performed a set of experiments to demonstrate that treatment of the counter electrode with SDBS is crucial for effective regeneration of nitrate ions in our capacitive system. To this end, we built and operated a comparison cell consisting of one CTA-AC electrode (as active electrode) and one untreated porous AC electrode (as counter electrode). Fig. 3 shows schematics of these two types of cells (i.e. the current cell with CTA-AC and DBS-AC electrodes; and the comparison cell with one CTA-AC electrode and an untreated AC electrode) during adsorption and short circuit regeneration. For simplicity of presentation, counter-ions (Na^+) are not shown here. Figure S2 of the SI shows measured effluent concentration and electric current under 0.8 V and 0 V external voltages for this comparison cell. The comparison cell exhibits negligible ion adsorption. For example, we estimate the comparison cell adsorbs only about 0.1 mg g^{-1} (mass of sodium nitrate removed per dry mass of both electrodes). By comparison, as we will describe in next Section, the i-CDI cell with both electrodes functionalized adsorbs about 6 mg g^{-1} under the same conditions. We hypothesize that this behavior is due to electrostatic adsorption of nitrate ions at the untreated counter electrode during regeneration. In the absence of negatively charged dodecyl benzene sulphonate (DBS) surfactant, and during regeneration step, nitrate ions expelled from active (negative, CTA-AC) electrode, likely adsorb into the counter (positive) electrode. We also hypothesize that, for the i-CDI cell with both electrodes treated, the negatively charged DBS surfactant electrostatically shields nitrate ions from adsorbing to the counter electrode. This aids in rejection of

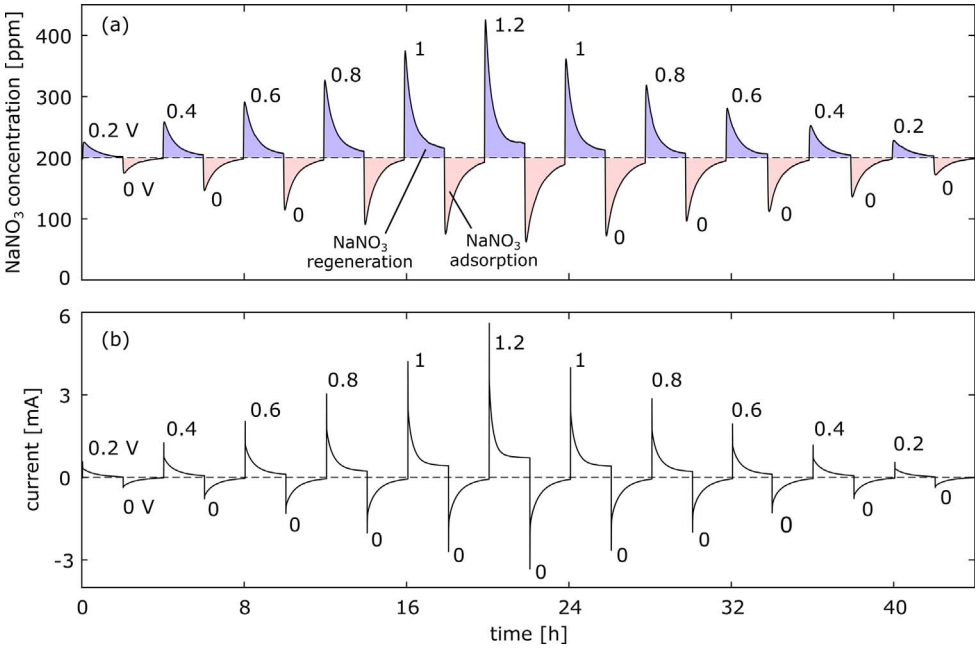

Fig. 2. Measured (a) effluent concentration (area under peaks is proportional to amount of nitrate adsorbed) and (b) electrical current for selected cycles of nitrate regeneration (at 0.2, 0.4, 0.6, 0.8, 1, and 1.2 V) and adsorption (at short-circuit). The applied voltage during the regeneration step electrostatically repels NO_3^- and Na^+ ions from the CTA-AC and DBS-AC functionalized electrodes, respectively. Results show an increase in effluent concentration baseline for > 1 V. This shift can be attributed mainly to effluent pH fluctuations due to Faradaic reactions. The subsequent short circuit discharges electrons from CTA-AC to DBS-AC (current is revered). The result is uptake of NO_3^- and Na^+ ions from solution into CTA-AC and DBS-AC electrodes during adsorption, and a subsequent electrostatic regeneration of adsorption capability.

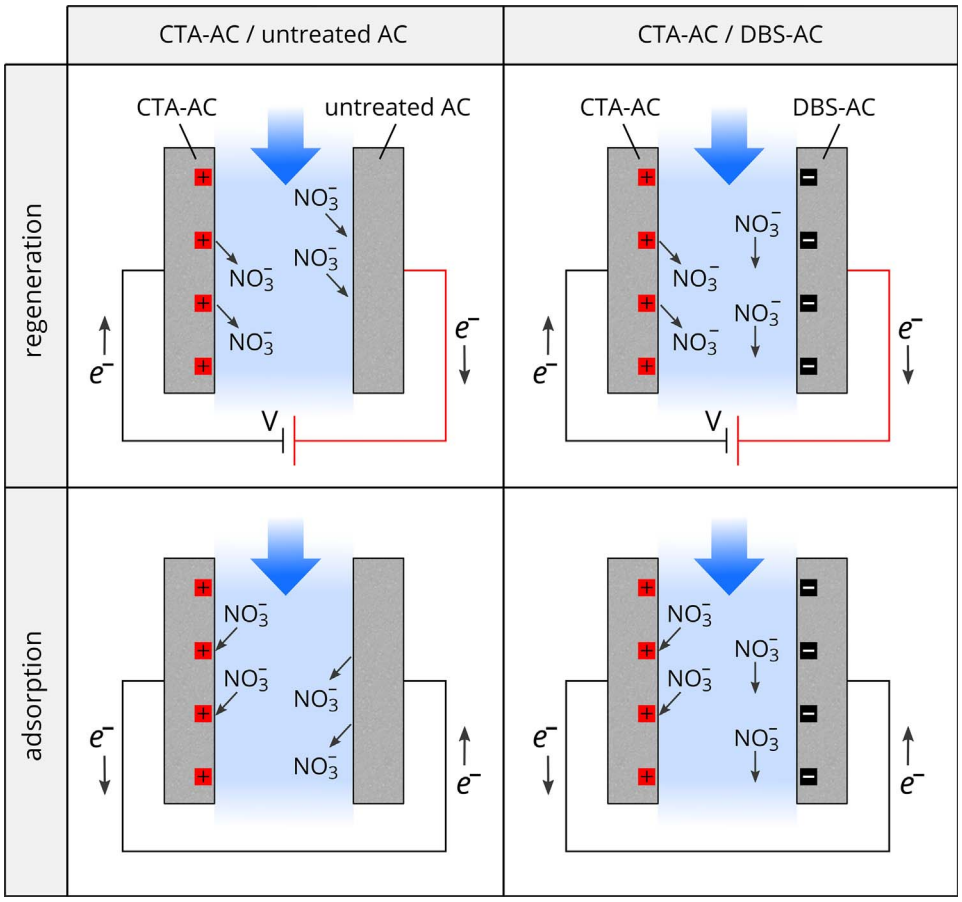

Fig. 3. Comparison between a CDI cell with untreated counter electrode (left column) and our i-CDI cell with both electrodes treated (right column). This comparison highlights the importance of counter electrode treatment with dodecyl benzene sulphonate (DBS) anionic surfactant for effective nitrate adsorption. In the absence of DBS (left column), nitrate electrostatically adsorbs to (is repelled from) untreated activated carbon counter electrode during regeneration (adsorption) step. Treatment of counter electrode with DBS (right column) likely electrostatically shields nitrate ions from entering the electrode. Note, counterions (Na^+) are not shown here for simplicity.

nitrate from the system in regeneration; and increases net adsorption of nitrate in the entire cycle.

3.3. Nitrate removal performance for cell with both electrodes functionalized

We here present salt adsorption and energy performance of our i-CDI cell. To this end, we applied 0 V for adsorption and 0.2–1.4 V (with 0.2 V increments) for the regeneration step, as mentioned in the Experimental setup section (see Section 2.2). The durations of adsorption and regeneration step were each 2 h (i.e. recovery ratio of 50%) and both were performed at the same 0.45 mL min^{-1} flow rate. Data of Fig. 2 was obtained from the same experiments which led to salt and energy calculations below (Figs. 4 and 5).

Fig. 4a shows experimental measurements of salt removal capacity of our cell as a function of regeneration voltage. The salt removal capacity is defined as mass of sodium nitrate removed (desorbed) in adsorption (regeneration) step per dry mass of both electrodes. Results show a linear increase in adsorption capacity (in absolute value) with regeneration voltage. Circles and diamonds respectively correspond to 2 h adsorption and 2 h regeneration step. The enhancement in adsorption with voltage is clear and suggests that higher regeneration voltages electrostatically repel more of the adsorbed ions; this in turn leaves more positively charged sites on CTA-AC electrode for the subsequent

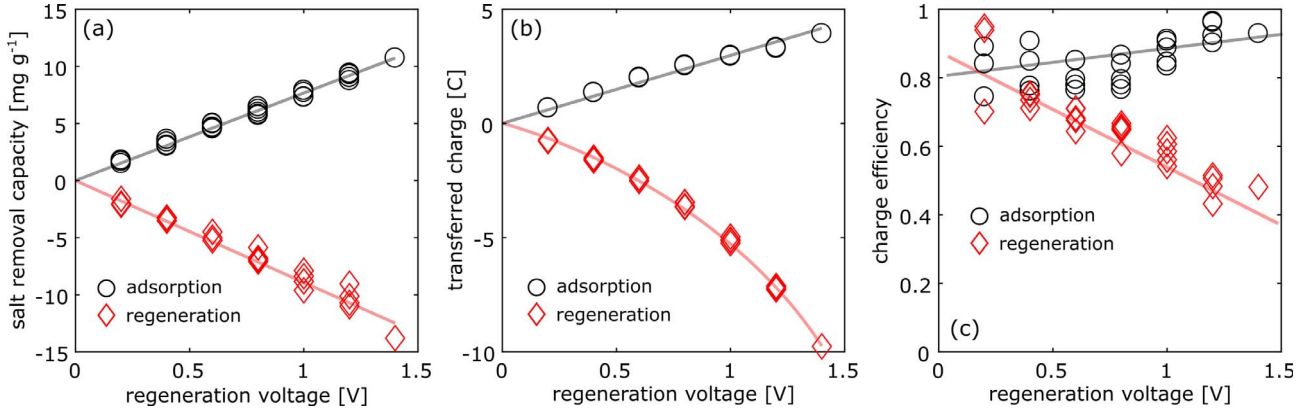

Fig. 4. (a) Salt removal capacity in units of mg of adsorbed sodium nitrate per g of both electrodes as a function of regeneration voltage. Circles and diamonds represent experimental measurements (time integrated) for 2 h adsorption and 2 h regeneration steps, respectively. Salt removal capacity increases linearly with voltage of regeneration step. (b) Transferred electronic charge during adsorption and regeneration steps. (c) Charge efficiency calculated as salt removed or regenerated (in units of Coulombs) divided by transferred charge. Solid lines serve to guide the eye.

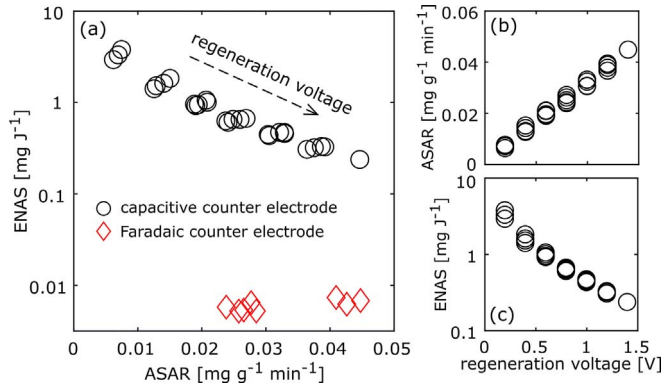

Fig. 5. (a) Coupling between nitrate adsorption rate (characterized by average salt adsorption rate, *ASAR*) and energy efficiency (characterized by energy-normalized adsorbed salt, *ENAS*) of capacitive DBS-AC counter electrode (this work) and titanium Faradaic counter electrode (Palko et al. [35]). Capacitive nitrate removal shows higher adsorption rate and energy efficiency. (b) *ASAR* and (c) *ENAS* as functions of regeneration voltage. Results show a tradeoff between the rate and energy efficiency of nitrate removal.

nitrate adsorption step. Results show up to around 10 mg g^{-1} sodium nitrate adsorption which corresponds to about 30% average concentration reduction.

Fig. 4b shows transferred electronic charge (in units of Coulombs) during adsorption and regeneration steps as a function of regeneration voltage. While adsorption capacity is similar (in magnitude) for adsorption and regeneration steps, the transferred charge is higher in regeneration step, mainly due to higher Faradaic reactions. This suggests that charge efficiency (defined as salt removed or regenerated (in units of Coulombs) divided by transferred charge) is greater for adsorption compared to regeneration. Fig. 4c summarizes calculated charge efficiency for data shown in Figs. 4a and 4b. The charge efficiency for adoption step (at 0 V) for our i-CDI cell is in 0.8–0.9 range and tends to increase with regeneration voltage (voltage applied at previous regeneration step). However, it decreases with voltage in regeneration step (diamond markers). This is expected because, as Fig. 4b suggests, Faradaic reactions are considerably higher in regeneration compared to adsorption. Solid lines here are to guide the eye.

We summarize our experimental study of the coupling between removal rate and energy efficiency in Fig. 5. Nitrate removal rate (in the adsorption step) can be quantified by average salt adsorption rate (*ASAR*) calculated as $(M_w Q/m_e t_{cycle}) \int (c_{in}-c_{out})dt$, where M_w is salt molecular weight, Q is flowrate, m_e is dry mass of both electrodes, t_{cycle} is total cycle time, and c_{in} and c_{out} are inlet and outlet concentrations, and the integration is performed over the duration of the adsorption [22,37]. The energy efficiency of the cycle is quantified by energy-normalized adsorbed salt (*ENAS*) calculated as $(M_w Q/E) \int (c_{in}-c_{out})dt$, where E is overall energy consumption in a cycle [37]. Note that E here is the energy consumption during the regeneration step (the short-circuit adsorption step does not recover energy). Markers in Fig. 5a each correspond to a single cycle (regeneration and adsorption). Circles show measured *ASAR* and *ENAS* for the experiments discussed in Section 2.2 and the arrow shows direction of increase of regeneration voltage. Diamond markers are data for preliminary experiments reported in Palko et al. [35] with titanium Faradaic counter electrode, applying open circuit adsorption and 3 V regeneration. Results show 1–2 orders of magnitude higher *ENAS*, indicating considerably more energy efficient nitrate removal with the capacitive cell (compared to the Faradaic cell). We estimate that the energy consumption is at most 0.07 kWh m^{-3} (energy per volume of purified water) at 1.4 V regeneration voltage with ~30% salt removal. Figs. 5b and 5c respectively show *ASAR* and *ENAS* (for the same experiments as in Fig. 5a) as functions of regeneration voltage. The two metrics have opposite trends: the adsorption rate increases almost linearly with regeneration voltage, while energy efficiency drops with voltage. This shows a clear tradeoff between desalination rate and energy efficiency of our cell; a concept observed in traditional CDI as well [37].

4. Conclusions

We presented a CDI cell with surface functionalized electrodes for nitrate removal which was operated under passive (at 0 V) adsorption followed by electrical regeneration. We functionalized the active electrodes with CTAB, a quaternary ammonium cationic surfactant, and we functionalized the capacitive counter electrode with SDBS anionic surfactant to enhance its cation adsorption capacity. The ability to electrically regenerate an active electrode provides potential advantages in terms of reduced maintenance costs and waste disposal needs. We showed that the adsorption capacity of the cell is linearly proportional to voltage applied during the previous regeneration step. We attribute this behavior to increased access to adsorption sites at higher regeneration voltages. We showed that replacing a Faradaic counter electrode by a capacitive counter electrode increases energy performance (*ENAS*) 1–2 orders of magnitude for the same adsorption rate (*ASAR*). Functionalized i-CDI systems have significant potential for high efficiency ionic pollutant removal with automated electrical regeneration and reduced waste disposal requirements.

Acknowledgements

We gratefully acknowledge funding from TomKat Center for Sustainable Energy at Stanford University. D.I.O would like to thank the support of CONICYT – Becas Chile fellowship no. 72160536. A.H. gratefully acknowledges the support from the Stanford Graduate Fellowship program of Stanford University.

Appendix A. Supplementary material

Supplementary data associated with this article can be found, in the online version, at http://dx.doi.org/10.1016/j.seppur.2017.11.027.

References

[1] R.F. Spalding, M.E. Exner, Occurrence of nitrate in groundwater—a review, J. Environ. Qual. 22 (1993) 392, http://dx.doi.org/10.2134/jeq1993.00472425002200030002x.
[2] Y. Zhang, F. Li, Q. Zhang, J. Li, Q. Liu, Tracing nitrate pollution sources and transformation in surface- and ground-waters using environmental isotopes, Sci. Total Environ. 490 (2014) 213–222, http://dx.doi.org/10.1016/j.scitotenv.2014.05.004.
[3] G. Gulis, M. Czompolyova, J.R. Cerhan, An ecologic study of nitrate in municipal drinking water and cancer incidence in Trnava District, Slovakia, Environ. Res. 88 (2002) 182–187, http://dx.doi.org/10.1006/enrs.2002.4331.
[4] K.H. Gelberg, L. Church, G. Casey, M. London, D.S. Roerig, J. Boyd, M. Hill, Nitrate levels in drinking water in rural New York State, Environ. Res. 80 (1999) 34–40, http://dx.doi.org/10.1006/enrs.1998.3881.
[5] A.M. Fan, V.E. Steinberg, Health implications of nitrate and nitrite in drinking water: an update on methemoglobinemia occurrence and reproductive and developmental toxicity, Regul. Toxicol. Pharmacol. 23 (1996) 35–43, http://dx.doi.org/10.1006/rtph.1996.0006.
[6] L. Knobeloch, K. Krenz, H. Anderson, C. Hovel, Methemoglobinemia in an infant—Wisconsin, Morb. Mortal. Wkly. Rep. 42 (1992) 217–219.
[7] P. Shahbazi, F. Vaezi, A. Hossein Mahvi, K. Naddaffi, A. Rahmani Reza, Nitrate removal from drinking water by point of use ion exchange, J. Res. Heal. Sci. 10 (2010) 91–97.
[8] S. Samatya, N. Kabay, Ü. Yüksel, M. Arda, M. Yüksel, Removal of nitrate from aqueous solution by nitrate selective ion exchange resins, React. Funct. Polym. 66 (2006) 1206–1214, http://dx.doi.org/10.1016/j.reactfunctpolym.2006.03.009.
[9] X. Xu, B. Gao, Y. Zhao, S. Chen, X. Tan, Q. Yue, J. Lin, Y. Wang, Nitrate removal from aqueous solution by Arundo donax L. reed based anion exchange resin, J. Hazard. Mater. 203–204 (2012) 86–92, http://dx.doi.org/10.1016/j.jhazmat.2011.11.094.
[10] G. Darracq, J. Baron, M. Joyeux, Kinetic and isotherm studies on perchlorate sorption by ion-exchange resins in drinking water treatment, J. Water Process Eng. 3 (2014) 123–131, http://dx.doi.org/10.1016/j.jwpe.2014.06.002.
[11] C.E. Harland, Ion Exchange: Theory and Practice, Royal Society of Chemistry, 2007.
[12] J. Bohdziewicz, M. Bodzek, E. Wąsik, The application of reverse osmosis and nanofiltration to the removal of nitrates from groundwater, Desalination 121 (1999)

139–147, http://dx.doi.org/10.1016/S0011-9164(99)00015-6.
[13] J.J. Schoeman, A. Steyn, Nitrate removal with reverse osmosis in a rural area in South Africa, Desalination 155 (2003) 15–26, http://dx.doi.org/10.1016/S0011-9164(03)00235-2.
[14] D.L. Shaffer, N.Y. Yip, J. Gilron, M. Elimelech, Seawater desalination for agriculture by integrated forward and reverse osmosis: improved product water quality for potentially less energy, J. Memb. Sci. 415–416 (2012) 1–8, http://dx.doi.org/10.1016/j.memsci.2012.05.016.
[15] C.E. Barrera-Díaz, V. Lugo-Lugo, B. Bilyeu, A review of chemical, electrochemical and biological methods for aqueous Cr(VI) reduction, J. Hazard. Mater. 223–224 (2012) 1–12, http://dx.doi.org/10.1016/j.jhazmat.2012.04.054.
[16] E.J. Bouwer, P.B. Crowe, Biological processes in drinking water treatment, Am. Water Work. Assoc. 80 (1988) 82–93.
[17] J.C. Farmer, D.V. Fix, G.V. Mack, R.W. Pekala, J.F. Poco, Capacitive deionization of NH4ClO4 solutions with carbon aerogel electrodes, J. Appl. Electrochem. 26 (1996) 1007–1018, http://dx.doi.org/10.1007/BF00242195.
[18] S.J. Seo, H. Jeon, J.K. Lee, G.Y. Kim, D. Park, H. Nojima, J. Lee, S.H. Moon, Investigation on removal of hardness ions by capacitive deionization (CDI) for water softening applications, Water Res. 44 (2010) 2267–2275, http://dx.doi.org/10.1016/j.watres.2009.10.020.
[19] Y. Oren, Capacitive deionization (CDI) for desalination and water treatment—past, present and future (a review), Desalination 228 (2008) 10–29, http://dx.doi.org/10.1016/j.desal.2007.08.005.
[20] A. Hemmatifar, M. Stadermann, J.G. Santiago, Two-dimensional porous electrode model for capacitive deionization, J. Phys. Chem. C 119 (2015) 24681–24694, http://dx.doi.org/10.1021/acs.jpcc.5b05847.
[21] H. Li, L. Zou, Ion-exchange membrane capacitive deionization: a new strategy for brackish water desalination, Desalination 275 (2011) 62–66, http://dx.doi.org/10.1016/j.desal.2011.02.027.
[22] M.E. Suss, S. Porada, X. Sun, P.M. Biesheuvel, J. Yoon, V. Presser, Water desalination via capacitive deionization: what is it and what can we expect from it? Energy Environ. Sci. 8 (2015) 2296–2319, http://dx.doi.org/10.1039/C5EE00519A.
[23] M. Andelman, Flow through capacitor basics, Sep. Purif. Technol. 80 (2011) 262–269, http://dx.doi.org/10.1016/j.seppur.2011.05.004.
[24] M.E. Suss, T.F. Baumann, W.L. Bourcier, C.M. Spadaccini, K.A. Rose, J.G. Santiago, M. Stadermann, Capacitive desalination with flow-through electrodes, Energy Environ. Sci. 5 (2012) 9511, http://dx.doi.org/10.1039/c2ee21498a.
[25] Y. Qu, P.G. Campbell, L. Gu, J.M. Knipe, E. Dzenitis, J.G. Santiago, M. Stadermann, Energy consumption analysis of constant voltage and constant current operations in capacitive deionization, Desalination 400 (2016) 18–24, http://dx.doi.org/10.1016/j.desal.2016.09.014.
[26] X. Gao, A. Omosebi, J. Landon, K. Liu, Surface charge enhanced carbon electrodes for stable and efficient capacitive deionization using inverted adsorption–desorption behavior, Energy Environ. Sci. 8 (2015) 897, http://dx.doi.org/10.1039/c4ee03172e.
[27] A. Hemmatifar, D.I. Oyarzun, J.W. Palko, S.A. Hawks, M. Stadermann, J.G. Santiago, Equilibria model for pH variations and ion adsorption in capacitive deionization electrodes, Water Res. (2017), http://dx.doi.org/10.1016/j.watres.2017.05.036.
[28] P.M. Biesheuvel, M.E. Suss, H.V.M. Hamelers, Theory of water desalination by porous electrodes with immobile chemical charge, Colloids Interf. Sci. Commun. 9 (2015) 1–5, http://dx.doi.org/10.1016/j.colcom.2015.12.001.
[29] X. Gao, A. Omosebi, J. Landon, K. Liu, Enhanced salt removal in an inverted capacitive deionization cell using amine modified microporous carbon cathodes, Environ. Sci. Technol. 49 (2015) 10920–10926, http://dx.doi.org/10.1021/acs.est.5b02320.
[30] W. Tang, P. Kovalsky, D. He, T.D. Waite, Fluoride and nitrate removal from brackish groundwaters by batch-mode capacitive deionization, Water Res. 84 (2015) 342–349, http://dx.doi.org/10.1016/j.watres.2015.08.012.
[31] N. Pugazhenthiran, S. Sen Gupta, A. Prabhath, M. Manikandan, J.R. Swathy, V.K. Raman, T. Pradeep, Cellulose derived graphenic fibers for capacitive desalination of brackish water, ACS Appl. Mater. Interf. 7 (2015) 20156–20163, http://dx.doi.org/10.1021/acsami.5b05510.
[32] Y.J. Kim, J.H. Choi, Selective removal of nitrate ion using a novel composite carbon electrode in capacitive deionization, Water Res. 46 (2012) 6033–6039, http://dx.doi.org/10.1016/j.watres.2012.08.031.
[33] Y.J. Kim, J.H. Kim, J.H. Choi, Selective removal of nitrate ions by controlling the applied current in membrane capacitive deionization (MCDI), J. Memb. Sci. 429 (2013) 52–57, http://dx.doi.org/10.1016/j.memsci.2012.11.064.
[34] J.-H. Yeo, J.-H. Choi, Enhancement of nitrate removal from a solution of mixed nitrate, chloride and sulfate ions using a nitrate-selective carbon electrode, Desalination 320 (2013) 10–16, http://dx.doi.org/10.1016/j.desal.2013.04.013.
[35] J.W. Palko, D.I. Oyarzun, B. Ha, M. Stadermann, J.G. Santiago, Nitrate removal from water using electrostatic regeneration of functionalized adsorbent, Chem. Eng. J. (2017), http://dx.doi.org/10.1016/j.cej.2017.10.161 (in press).
[36] M. Andelman, Ionic group derivitized nano porous carbon electrodes for capacitive deionization, J. Mater. Sci. Chem. Eng. 2 (03) (2014) 16, http://dx.doi.org/10.4236/msce.2014.23002.
[37] A. Hemmatifar, J.W. Palko, M. Stadermann, J.G. Santiago, Energy breakdown in capacitive deionization, Water Res. 104 (2016) 303–311, http://dx.doi.org/10.1016/j.watres.2016.08.020.
[38] S. Shanbhag, J.F. Whitacre, M.S. Mauter, The origins of low efficiency in electrochemical de-ionization systems, J. Electrochem. Soc. 163 (2016) E363–E371, http://dx.doi.org/10.1149/2.0181614jes.